

Functionalization of Multi-walled Carbon Nanotubes–Silver Nanoparticle (MWCNTs-AgNPs) as a Drug Delivery System for Ibuprofen

Murni Handayani ^{a,1}, Geolita Ihsantia Ning Asih ^b, Triana Kusumaningsih ^b, Yuni Kusumastuti ^{c,2}, Rochmadi ^c

^a Research Center for Metallurgy and Materials, National Research and Innovation Agency (BRIN), PUSPIPTEK Area, Building 470, Tangerang Selatan, Banten, 15314, Indonesia

^b Department of Chemistry, Faculty of Mathematics and Natural Sciences, Sebelas Maret University, Surakarta, 57126, Indonesia

^c Chemical Engineering Department, Faculty of Engineering, Universitas Gadjah Mada, Jl. Grafika 2, Yogyakarta, 55281, Indonesia

Corresponding author: ¹murni.handayani@lipi.go.id, ²yuni_kusumastuti@ugm.ac.id

Abstract—Nanoparticle utilization for the prevention, diagnostics, and treatment of diseases is widely known as one of the medicine branches, nanomedicine. The ability to penetrate the higher space between cells and cell walls makes nanoparticles have the potential to be used as a drug delivery system (DDS). Furthermore, various techniques can be combined with nanoparticles due to their flexibility. AgNPs are one of the interesting nanoparticles to be developed into DDS. It is because they can improve antibacterial, antiviral, antifungal, antioxidant, and physicochemical properties. In addition, AgNPs have biocompatibility that can improve drug delivery capability. On the other hand, carbon-based nanomaterials such as MWCNTs have unique properties that can be potentially used as composite materials for application as DDS. Therefore, to increase the ability of DDS, the in-situ synthesis of MWCNT-AgNPs nanocomposites was carried out. UV-Vis observed the absorption peak of the nanocomposite. The characterization of the crystal structure was performed using XRD. FESEM-EDX conducted the determination of the morphology of nanocomposite and the chemical composition. The distribution of AgNPs on the MWCNTs surface was performed by TEM. Furthermore, Raman spectroscopy was used to investigate the vibration of the MWCNT-AgNPs. Drug Loading was performed using UV-Vis measurements. The results showed that MWCNT-AgNPs as a DDS are successfully created in the drug loading stage. Drug loading stage properties are increased with the increasing loading time of Ibuprofen on MWCNT-AgNPs. The optimum percentage of drug loading for Ibuprofen by MWCNTs-AgNPs was 43.7% in a contact time of 27 hours.

Keywords— Multi-walled carbon nanotubes; silver nanoparticles; drug delivery system (DDS); ibuprofen.

Manuscript received 23 Mar. 2021; revised 5 May 2021; accepted 30 Aug. 2021. Date of publication 30 Apr. 2022. IJASEIT is licensed under a Creative Commons Attribution-Share Alike 4.0 International License.



I. INTRODUCTION

Nanomedicine is a branch of medicine that utilizes nanomaterials to prevent, diagnose, and treat diseases. The use of nanomaterials in the health sector is expected to become drug carrier devices that can increase the effectiveness and safety of the drug by reducing toxicity and side effects [1]. Nanotechnology produces materials of various types at a nanoscale level called nanoparticles. At the nanoscale, man-made materials may show unique properties that differ from bulk materials. Nanoparticles have small sizes (between 1-100 nm), large surface area, and unique surface characteristics. The uniqueness of nanoparticles includes their conductivity, catalytic, fire resistance, water-repellent, and anti-rust properties [2], [3]. Their nanoscale size and unique

properties allow nanoparticles to be developed in diagnostic applications using imaging technology and medicinal purposes through drug delivery technologies. Nanoparticles are composed of metallic atoms, nonmetals, or alloy. Nanoparticles consist of different structures that vary from nanorods, nanotubes, nanoshells, quantum dots, liposomes, polymers, dendrimers, and micelle [4], [5].

Nanoparticles can be used as a drug delivery system (DDS)[6]. DDS is a formula used to deliver a drug to a specific part of the body at a certain rate. So that it reaches an effective concentration for the drug's action. DDS that utilizes nanoparticles provides optimal delivery targets with reduced side effects and toxicity, whereby an active moiety is conveyed explicitly to the site of action by naocarriers [7]. Nanoparticles can be used as DDS because they can reach the

target site with a reduced dose frequency in a controlled manner, thereby reducing toxicity and adverse side effects. This is because drug delivery in the nanoscale can adjust drug release rates, increase the permeability of biological membranes, change the distribution of the drug in vivo, and increase their efficiency through encapsulation, absorption, and even covalent cross-linking.

Furthermore, nanoparticles have the flexibility to be combined with various other technologies. Therefore, nanoparticle as DDS has the potential to be developed[8]–[11]. Metal-based nanoparticles have a smaller size so that they have selectivity for bacteria and can be against pathogens. Metal-based nanoparticles have a non-specific bacterial toxicity mechanism that can broaden the spectrum of antibacterial activity [12]. One of the metallic nanoparticles that can be used as DDS is silver nanoparticles (AgNPs). Silver can be used to manufacture nanoparticles because it has antibacterial, antiviral, antifungal, antioxidant, anti-inflammatory, and physicochemical properties that can be increased [7], [13]. This remarkable antimicrobial activity in silver nanoparticles is due to the large surface-volume ratio. AgNPs contain 20 to 15,000 silver atoms, and their diameters are less than 100 nm. AgNPs have potential in biomedical applications, such as drug delivery, medical imaging, and molecular diagnostics. This occurs because AgNPs have shown low cytotoxicity and immunological responses [14]–[16]. AgNPs have cell chemical stability, high conductivity, catalytic activity, and localized surface plasma resonance and thus have vast potential in the medical field and can be used as therapeutic agents [17].

Carbon-based nanomaterials have unique properties such as electrical, thermal, mechanical, and chemical. Thus it has high potential as composite materials and drug delivery[18]. One of the most well-known carbon-based nanomaterials is Carbon nanotubes (CNT), one of the allotropes of 3D carbon. A CNT is defined as a cylinder composed of graphene sheets rolled to form a tube with a nanometer-scale diameter, with a cap at both ends [19]. The uniqueness of CNT includes superior mechanical, electrical, and thermal properties, thus making them ideal for the manufacture of nanostructured composites. The excellent mechanical properties of CNT are due to the presence of carbon bonds sp^2 [20]. The sp^2 hybridization gives CNT a mechanical strength that is even stronger than the sp^3 bond in a diamond. CNT consists of two types: Single-walled Carbon Nanotubes (SWCNT) and Multi-walled Carbon Nanotubes (MWCNT). Multi-walled carbon nanotubes (MWCNT) are CNT types that consist of several graphite sheets that roll coaxially and regularly. MWCNT consists of several graphene sheets rolled with a gap between the graphene interlayer of MWCNT measures approximately 0.34 nm on average[21], [22]. MWCNT is easy to modify and functionalize due to an increase in the number of layers in MWCNT, increasing the number of defects [23]. Carbon Nanotubes exhibit some unique features because of their unique special 1D structure, and they possess advantageous properties, such as superior mechanical strength and good thermal conductivity. The report by Iijima on carbon nanotubes in 1991 renewed the interest in carbon-based nanomaterials. CNT are widely used in biotechnological and biomedical applications, such as biosensors, drug delivery, tissue engineering, and cancer cell death. This occurs because

CNT has unique characteristics to be applied as a drug delivery system due to their nano-sized diameter, hollow structure, unique atomic configuration, and excellent physicochemical properties, such as intrinsic stability, structural flexibility, and the ability to prolong the circulation time and hence, the bioavailability of the carried drug molecules. In addition, CNT also has good electricity, good thermal conductivity, and the ability to penetrate living cells without causing damage or death, which makes them suitable nanocarriers for drug delivery [18], [24]–[28]. The superiority of MWCNT based DDS is that it can easily cross the cytoplasmic membrane and nuclear membrane so that the drug carried by MWCNT can be released in the target cell at the intact concentration [29].

One silver metal is catalytically active with carbon support, such as graphene oxide, carbon nanotubes, and activated carbon[30]. In this work, we present an in-situ method of functionalized MWCNT-AgNPs composites. The MWCNT-AgNPs composites formed were observed for their ability to drug loading in applications as a drug delivery system (DDS) for Ibuprofen. To the best of our knowledge, there is no report on drug delivery systems using MWCNT-AgNPs nanocomposites for drug loading for Ibuprofen.

II. MATERIALS AND METHOD

A. Materials

MWCNT powder was purchased from Cheap Tubes Inc, USA (20-40 nm diameter, 10-20 μ m length, > 90% purity), 95-97% sulfuric acid (H_2SO_4) solution, nitric acid solution (HNO_3) 65%, distilled water, $AgNO_3$ solution, and NaOH solution. The drug loading ability test was carried out using Ibuprofen.

B. Methods

1) *Functionalization of Multi-walled Carbon Nanotubes (MWCNT)*: The functionalization of MWCNT was prepared by refluxing pure MWCNT in strong acid ($H_2SO_4 : HNO_3$) with a ratio of 3: 1. The amount of 4.001 grams of MWCNT were added by 75 mL of H_2SO_4 95-97% and 25 mL of HNO_3 65%, then refluxed for 7 hours with a magnetic stirrer at a temperature of 32°C. The result is diluted with 1200 mL distilled water or until it is cold and dilute. The mixture was precipitated by gravity to obtain a black precipitate. The precipitate was washed with distilled water using a centrifuge until the filtrate pH was neutral. The neutralized precipitate was transferred to crucible porcelain and dried in an oven at 80°C.

2) *Synthesis of MWCNT-AgNPs Composite*: The MWCNT-AgNPs composites were synthesized by sonication process of 0.501 grams MWCNT-COOH with 200 mL distilled water for 1 hour. The suspension was added by 200 mL of 0.1 M $AgNO_3$ and sonicated again for 30 minutes. After sonication, the suspension was stirred and heated until 85°C. When the solution temperature reached 85°C, 25 mL 8 M NaOH was added slowly and stirred for 10 minutes with the constant temperature at 85°C. The solution was then washed with distilled water using a centrifuge until the pH of the filtrate was neutral. The precipitate was dried in an oven at 80°C.

3) *Characterization of Composites*: The maximum wavelengths of MWCNT, MWCNT-COOH, and MWCNT-AgNPs composites were characterized by UV-Vis spectrophotometer (UV-Vis, LABTRON LUS B-12). The crystal structure characterization of MWCNT-COOH and MWCNT-AgNPs composites was carried out using X-ray Diffraction (diffraction (XRD, Smartlab Rigaku X-ray diffraction) with Cu-K α radiation ($\lambda= 1.5406 \text{ \AA}$). Surface morphology and analysis of MWCNT-COOH and MWCNT-AgNPs composites were characterized by Field Emission Scanning Electron Microscopy-Energy Dispersive X-ray Spectroscopy (FESEM-EDX, QUANTA 650), the nanostructure of MWCNTs-AgNPs was characterized by Transmission Electron Microscope (TEM, TECNAI G220 S-TWIN). The vibration spectra of MWCNTs were performed using Raman spectroscopy (Labspec 6-HORIBA Scientific Type iHR320).

4) *Application of MWCNT-AgNPs Composite as Drug Delivery System (DDS)*: The drug loading stage in DDS was analyzed by comparing the results of the UV-Vis spectrophotometer between the Ibuprofen loading on the MWCNT-AgNPs composites with the standard solution of Ibuprofen. Preparation of standard solutions was carried out by sonication of fine Ibuprofen in 10 mL of distilled water. Standard solutions are made with 3 mass variations of Ibuprofen, namely 2 mg, 3 mg, and 4 mg. The drug loading ability for Ibuprofen by the MWCNT-AgNPs composite was carried out by stirring 5 mg of Ibuprofen and 10 mg of MWCNT-AgNPs composite in 20 mL of distilled water. The solution was stirred with various time variations: 3 hours, 6 hours, 24 hours, and 27 hours. The percentage of drug loading was measured by UV-Vis spectrophotometer with a wavelength of 264 nm, using the equation: Drug Loading (%) = $(C_0 - C_t / C_0) \times 100$.

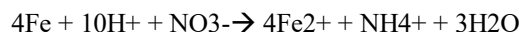
III. RESULTS AND DISCUSSION

A. Functionalization of Multi-walled Carbon Nanotubes (MWCNT)

The MWCNT functionalization aims to remove residuary catalyst particles and impurities (i.e., Fe metal, ferrocene, and un-pyrolyzed benzene residue) that are formed from the MWCNT synthesis stage. Besides that, the MWCNT functionalization aims to remove amorphous carbon and increase the MWCNT surface area due to defects or cavities. In addition, the purpose of the functionalization of MWCNT is to change the characteristics of MWCNT from hydrophobic to hydrophilic with the addition of a hydroxyl functional group. This step is crucial because the properties of the nanomaterials generally have hydrophobic properties, resulting in these nanomaterials not forming stable suspensions in aqueous media. The functional groups formed through the oxidation process can stabilize MWCNT. MWCNT can be functionalized with a specific chemical species to add a functional group on them using various types of acids and acid mixtures, such as HNO₃, H₂SO₄/HNO₃, HCl/H₂SO₄/HNO₃, H₂O₂, KMnO₄, K₂Cr₂O₇/H₂SO₄, and KMnO₄/H₂SO₄[31], [32].

HNO₃ solution is used as a washing solution because it is a strong acidic and a strong oxidizing agent which ionizes easily into H⁺ and NO₃⁻. Furthermore, the HNO₃ solution is

easily evaporated and does not dissolve or damage the MWCNT structure. The functionalization process is carried out using the reflux method because the oxidation of HNO₃ depends on the temperature of the solution, where the temperature will affect the efficiency and effectiveness of the functionalization reaction. The reflux method will release Fe particles and cause defects on the MWCNT walls due to nitric acid. Consequently, the addition of strong acid is needed. The addition of a strong acid mixture such H₂SO₄ and HNO₃ in the functionalization process will open the tubes which function to bind chemicals at the defect site, such as the formation of carboxylic groups (-COOH). Functionalization improves their wettability and enables their dispersion in polar media[33], [34].



B. Spectrophotometer UV-Vis Analysis Result

The UV-Vis spectrophotometer analysis of MWCNT, MWCNT-COOH, and MWCNT-AgNPs are shown in Figure 1. The purple line shows the characterization result of MWCNT, which is indicated by a low absorption peak at a maximum wavelength of $\sim 220 \text{ nm}$. MWCNT-COOH characterization result is marked with a red line on the spectra, where there is one peak with a maximum wavelength of 261 nm. The peak is the π - π^* transition of the C-C aromatic ring[35]. The analysis results of the MWCNT-AgNPs composite (blue line) show that there is a characteristic peak of MWCNT at a maximum wavelength of 200 nm to 250 nm and there is a peak at a wavelength of $\sim 260 \text{ nm}$. The analysis of the MWCNT-AgNPs composites using a UV-Vis spectrophotometer did not show any peak characteristics of Ag at a wavelength of 406 nm. These results will then be supported by the characterization of MWCNT-AgNPs composites using XRD and SEM-EDX.

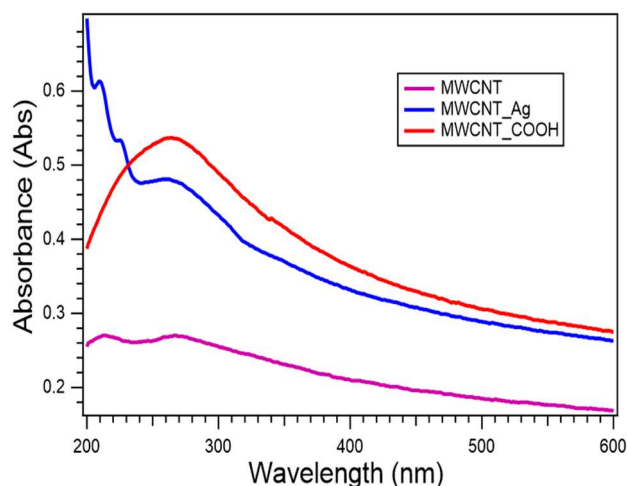


Fig. 1 Spectrophotometer Result UV-Vis of MWCNT, MWCNT-COOH, and MWCNT-AgNPs.

C. X-ray Diffraction Characterization Result

Analysis using XRD was carried out in order to characterize the crystals structure of MWCNT-COOH and MWCNT-AgNPs. The results of the XRD analysis of the MWCNT-COOH are shown in Figure 2.

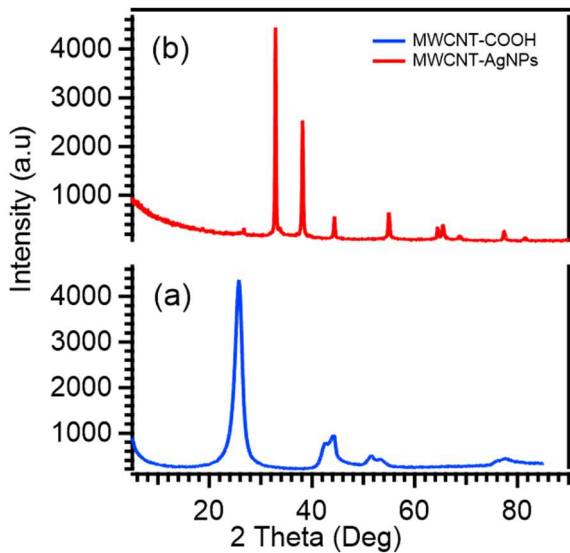


Fig. 2 XRD Characterization of (a) MWCNT-COOH and (b) MWCNT-AgNPs

The result of MWCNT-COOH characterization in Figure 2a. shows the presence of MWCNT peaks at $2\theta \sim 25.7^\circ$ and $\sim 44.2^\circ$ with the main plane (002), and the additional plane (100). MWCNT has different chirality, consists of different layers and shows the same diffraction pattern in-plane (002) with graphite sheet. The peak (100) is formed due to the curved nature of the nanotubes[36].

Figure 2b shows the diffractogram results of the analysis of the MWCNT-AgNPs composite using XRD. The results of the analysis indicated the presence of Ag peaks at 2θ between 30° and 40° . However, the main plane MWCNT peak (002) only appeared as a small, indistinct diffractogram at $2\theta \sim 25.7^\circ$. The MWCNT diffractogram on the MWCNT-AgNPs composites is strengthened by the results of XRD analysis from MWCNT-COOH in Figure 2a.

D. Scanning Electron Microscopy-Energy Dispersive X-ray Spectroscopy Characterization Result

Analysis using SEM aims to determine the morphology of a material. This analysis can be combined with EDX as support to determine the chemical composition and % mass and % of atoms contained in the material. In order to enhance the morphology in the characterization, SEM-EDX analysis was performed by coating the samples of MWCNT-COOH and MWCNT-AgNPs with Au.

The results of the FESEM-EDX characterization of functionalized MWCNT-COOH and MWCNT-AgNPs is shown in Figure 3. SEM visualization is used to study the morphology of MWCNT-COOH, where the purified MWCNT will have a more regular and uniform morphology. The reflux process using strong acids can reduce the Fe adhering to the tip of the MWCNT surface and reduce amorphous carbon that is not in the nanotubes form.

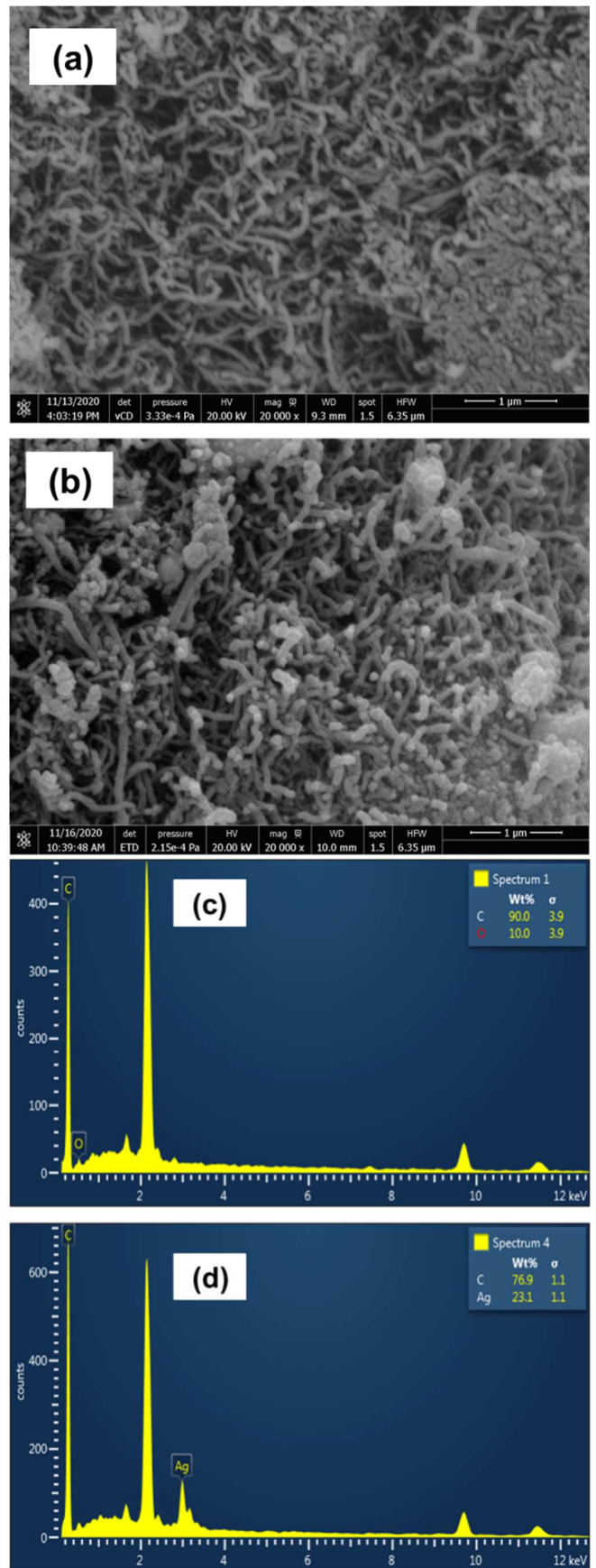


Fig. 3 (a) SEM Characterization of MWCNT-COOH in 20,000x magnification and (b) SEM Characterization of MWCNT-AgNPs in 20,000x magnification. (c) EDX Characterization of MWCNT-COOH and (d) EDX Characterization of MWCNT-AgNPs

TABLE I
FESEM-EDX COMPOSITION RESULT OF MWCNT-COOH

Compound	keV	% Mass	% Atom
C	0.277	89.95	92.26
O	0.525	10.05	7.74

Based on the EDX characterization data shown in Table 1, there is no Fe element in MWCNT-COOH. This indicates that the Fe from the previous MWCNT synthesis has been completely separated from MWCNT. Carbon and little oxygen element were found in the EDX analysis of MWCNT. The presence of O element is due to the carboxylate group (-COOH) formed in the MWCNT functionalization process. The smaller the amount of Fe attached to the surface tip of MWCNT-COOH, the smaller the toxicity level of MWCNT, which will increase the character of MWCNT-COOH corresponding to compatibility applications.

The results of FESEM-EDX characterization of the MWCNT-AgNPs composite can be seen in Figures 3b and 3d. Based on the results of the MWCNT-AgNPs morphological visualization using FESEM, it can be seen obviously that AgNPs are homogeneously distributed into the MWCNTs matrix, which is shown as spherical shape and bright image of silver nanoparticles. These results are supported by data from EDX analysis which proves that the MWCNT-AgNPs composites have been successfully formed, marked by the presence of the C element from MWCNT and the Ag element, which is from AgNPs, where the mass percentage and atomic percentage can be seen in Table 2.

TABLE II
FESEM-EDX COMPOSITION RESULT OF MWCNT-AGNPS

Compound	keV	% Mass	% Atom
C	0.277	76.95	96.77
Ag	2.983	23.05	3.23

E. Transmission Electron Microscopy (TEM) Analysis Result of MWCNT-AgNPs

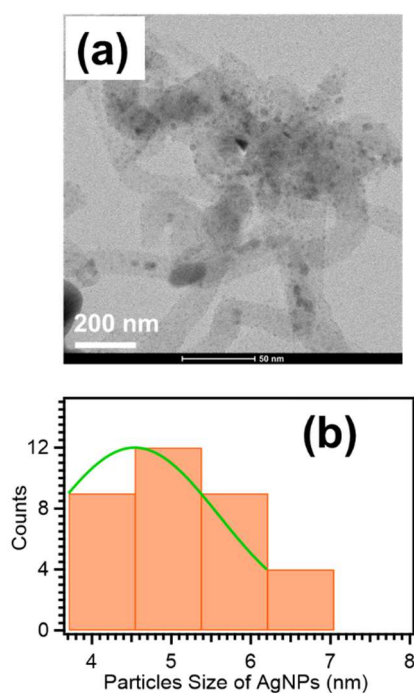


Fig. 4 (a) TEM analysis Result of MWCNT-AgNPs in scale bar of 200 nm, (b) Particle size distribution of MWCNT-AgNPs

The TEM images of MWCNTs-AgNPs are demonstrated in Figures 4 (a). The presence of silver nanoparticles distributed on the surface of MWCNT is indicated by the small particles with a diameter of 3 – 7 nm and the particles size distribution of AgNPs calculated by ImageJ exhibiting a mean diameter of $4.66 \text{ nm} \pm 0.84$ (Figure 4.b). The structure of MWCNT has an average diameter of 15-30 nm. It is observed that AgNPs tend to present onto the surface of agglomerated MWCNT compared with the surface of individual MWCNT. The increasing AgNPs distributed on the surface of MWCNT cause bent the structure of MWCNT due to a high tendency to aggregation of AgNPs to form clusters of silver nanoparticles.

It is confirmed from TEM image that no isolated AgNPs appear around MWCNTs. This indicates that silver nanoparticles can be self-assembled on the functionalized MWCNT. This reveals that the surface functionalization of MWCNT enhances the surface binding sites and the dispersion. Moreover, strong chemical oxidation of MWCNT using $\text{H}_2\text{SO}_4/\text{HNO}_3$ causes carboxyl groups on the MWCNT surface, allowing the interaction of Ag^+ with carbonyl groups to form the nucleation AgNPs on the surface of MWCNT[37].

F. Raman Spectroscopy Result of MWCNT-AgNPs

In order to get insights into the functionalization of MWCNTs, Raman spectroscopy has been applied to investigate the vibration of the MWCNT-AgNPs. It is shown in Figure 5. There are two prominent peaks with high intensity of Raman spectra of MWCNTs: the D band showing the defect structure observed at 1349.9 cm^{-1} and the G band showing graphite structure at 1586 cm^{-1} , respectively.

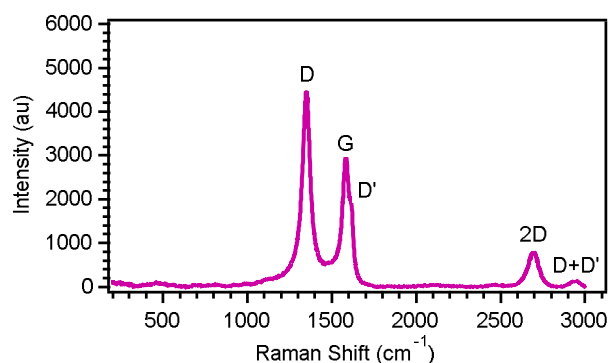


Fig. 5 Raman Spectra Result of MWCNT-AgNPs

It appears from the Raman spectra of MWCNTs-AgNPs that the intensity of the D band is higher than that of the intensity of the G band. The I_D/I_G ratio obtained from the calculation of I_D/I_G (MWCNT-AgNPs) is $4470/2969 = 1.50$, which has a good agreement with the previous work reported by Yusliza, Y., et.al.[38] The I_D/I_G ratio of MWCNT-AgNPs is higher than that of pristine MWCNTs, which exhibits that the distribution of AgNPs on the surface of MWCNTs causes defects in the MWCNTs structure[37]. The presence of a small D' band as a shoulder peak on the right side of the G band escalates the D band's intensity owing to the increasing disorder of graphite structures. Besides that, the existence of 2D band at 2690 cm^{-1} indicates the two phonons scattering which is susceptible to the purity and the defect of the MWCNTs [38].

G. Application of MWCNT-AgNPs Composites as Drug Delivery System (DDS)

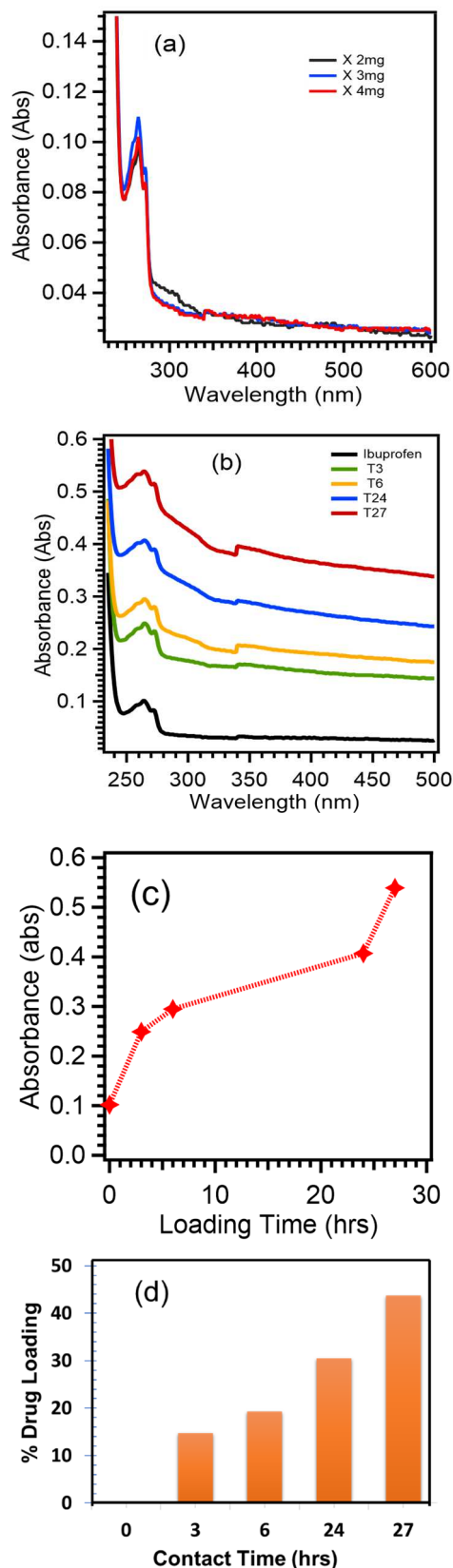


Fig. 6 Application of MWCNTs-AgNPs as DDS for Ibuprofen (a) Standard solution of Ibuprofen with mass of 2, 3 and 4 mg (b) Relationship between wavelength absorbance of ibuprofen loading on MWCNT-AgNPs at 3, 6, 24 and 27 hours, (c) Correlation between loading times with absorbance, (d) Relationship between Contact time with % drug loading of Ibuprofen.

Figure 6 (a) shows the standard solution of Ibuprofen with the 2, 3 and 4 mg of the mass. Comparing Ibuprofen standard solution and Ibuprofen loading on MWCNT-AgNPs characterization with time variations 3 hours, 6 hours, 24 hours, and 27 hours (denoted as T3, T6, T24, and T27) is depicted in Figure 6 (b).

Based on the characterization results from UV-Vis spectrophotometer depicted in Figure 6 (a-b). It can be seen that the loading results at each time variation have the same results of the maximum peak of absorbance at the wavelength of 264 nm, which are the same peaks observed in the standard ibuprofen solution (Figure 6.a), so it can be said that the MWCNT-AgNPs composites can be used for loading drugs in DDS. Figure 6 (b) shows the increase in the absorbance value of the maximum wavelength obtained from drug loading on MWCNT-AgNPs with various time variations. The curve that continues to increase at each time shows that the longer the Ibuprofen's loading process on MWCNT-AgNPs, the more absorbance is escalated (Figure 6.c), and this result indicates that MWCNT-AgNPs composites are effective as DDS of Ibuprofen. The drug loading percentage for ibuprofen solution by MWCNTs-AgNPs was 14.7%, 19.3%, 30.5%, and 43.7% in contact time of 3, 6, 24 and 27 hours, respectively (Figure 6.d).

IV. CONCLUSION

The MWCNT-AgNPs composites were successfully synthesized with in situ process. The results were confirmed by UV-Vis, XRD, and SEM-EDX spectrophotometers analysis. The MWCNT-AgNPs obtained are used for loading drugs in applications as a drug delivery system (DDS). Based on the results of UV-Vis spectra, there is a peak similarity between the ibuprofen standard solution and the ibuprofen loading on MWCNT-AgNPs, which indicates that MWCNT-AgNPs can be very potential for drug loading in applications as DDS. The performance of the MWCNT-AgNPs composite as DDS at the drug loading stage increased along with the increasing drug loading time.

ACKNOWLEDGMENT

We thank Research Center for Metallurgy and Materials (RCMM), National Research and Innovation Agency (BRIN), for this research's experimental facilities and support. We also acknowledge sophisticated analytical instrumentation facility from ELSA (E-Layanan Sains) – National Research and Innovation Agency (BRIN) to characterize the materials. In addition, we acknowledge partial research funding (contract number: 2808/UN1.DITLIT/DIT-LIT/PT/2020) from collaboration research between RCMM BRIN and UGM.

REFERENCES

- [1] M. A. Badea, M. Prodana, A. Dinischiotu, C. Crihana, D. Ionita, and M. Balas, "Cisplatin loaded multi-walled carbon nanotubes induce resistance in triple negative breast cancer cells," *Pharmaceutics*, vol. 10, no. 4, pp. 1–25, 2018, doi: 10.3390/pharmaceutics10040228.
- [2] I. Khan, K. Saeed, and I. Khan, "Nanoparticles: Properties, applications and toxicities," *Arab. J. Chem.*, vol. 12, no. 7, pp. 908–931, 2019, doi: 10.1016/j.arabjc.2017.05.011.
- [3] R. Gupta and H. Xie, "Nanoparticles in Daily Life: Applications, Toxicity, and Regulations," *J. Environ. Pathol. Toxicol. Oncol.*, vol. 37, no. 3, pp. 209–230, 2018, doi: 10.1615/JEnvironPatholToxicolOncol.2018026009.

- [4] M. Manzano and M. Vallet-Regí, "Mesoporous Silica Nanoparticles for Drug Delivery," *Adv. Funct. Mater.*, vol. 30, no. 2, pp. 3–5, 2020, doi: 10.1002/adfm.201902634.
- [5] I. X. Yin, J. Zhang, I. S. Zhao, M. L. Mei, Q. Li, and C. H. Chu, "The antibacterial mechanism of silver nanoparticles and its application in dentistry," *Int. J. Nanomedicine*, vol. 15, pp. 2555–2562, 2020, doi: 10.2147/IJN.S246764.
- [6] L. Hajiaghhabaee, M. Eslambolipour, A. Badiei, M. R. Ganjali, and G. M. Ziarani, "Controlled release of anticancer drug using o-phenylenediamine functionalized SBA-15 as a novel nanocarrier," *Chem. Pap.*, no. 0123456789, pp. 1–10, 2020, doi: 10.1007/s11696-020-01422-9.
- [7] N. Aminu, I. Bello, N. M. Umar, N. Tanko, A. Aminu, and M. M. Audu, "The influence of nanoparticulate drug delivery systems in drug therapy," *J. Drug Deliv. Sci. Technol.*, vol. 60, no. July, p. 101961, 2020, doi: 10.1016/j.jddst.2020.101961.
- [8] D. Lombardo, M. A. Kiselev, and M. T. Caccamo, "Smart Nanoparticles for Drug Delivery Application: Development of Versatile Nanocarrier Platforms in Biotechnology and Nanomedicine," *J. Nanomater.*, vol. 2019, pp. 1–26, 2019, doi: 10.1155/2019/3702518.
- [9] Y. Ye, X. Mao, J. Xu, J. Kong, and X. Hu, "Functional graphene oxide nanocarriers for drug delivery," *Int. J. Polym. Sci.*, vol. 2019, pp. 1–7, 2019, doi: 10.1155/2019/8453493.
- [10] N. Tyagi, Y. H. Song, and R. De, "Recent progress on biocompatible nanocarrier-based genistein delivery systems in cancer therapy," *J. Drug Target.*, vol. 27, no. 4, pp. 394–407, 2019, doi: 10.1080/1061186X.2018.1514040.
- [11] J. Zhao, Y. Wang, Y. Ma, Y. Liu, B. Yan, and L. Wang, "Smart nanocarrier based on PEGylated hyaluronic acid for deacetyl mycoepoxydience: High stability with enhanced bioavailability and efficiency," *Carbohydr. Polym.*, vol. 203, no. June 2018, pp. 356–368, 2019, doi: 10.1016/j.carbpol.2018.09.071.
- [12] E. Sánchez-López *et al.*, "Metal-based nanoparticles as antimicrobial agents: An overview," *Nanomaterials*, vol. 10, no. 2, pp. 1–39, 2020, doi: 10.3390/nano10020292.
- [13] X. Liu, P. Gao, J. Du, X. Zhao, and K. K. Y. Wong, "Long-term anti-inflammatory efficacy in intestinal anastomosis in mice using silver nanoparticle-coated suture," *J. Pediatr. Surg.*, vol. 52, no. 12, pp. 2083–2087, 2017, doi: 10.1016/j.jpedsurg.2017.08.026.
- [14] M. Oves *et al.*, "Antimicrobial and anticancer activities of silver nanoparticles synthesized from the root hair extract of Phoenix dactylifera," *Mater. Sci. Eng. C*, vol. 89, pp. 429–443, 2018, doi: 10.1016/j.msec.2018.03.035.
- [15] M. S. Samuel, S. Jose, E. Selvarajan, T. Mathimani, and A. Pugazhendhi, "Biosynthesized silver nanoparticles using *Bacillus amyloliquefaciens*; Application for cytotoxicity effect on A549 cell line and photocatalytic degradation of p-nitrophenol," *J. Photochem. Photobiol. B Biol.*, vol. 202, p. 111642, 2020, doi: 10.1016/j.jphotobiol.2019.111642.
- [16] A. Pugazhendhi, T. N. J. I. Edison, I. Karuppusamy, and B. Kathirvel, "Inorganic nanoparticles: A potential cancer therapy for human welfare," *Int. J. Pharm.*, vol. 539, no. 1–2, pp. 104–111, 2018, doi: 10.1016/j.ijpharm.2018.01.034.
- [17] H. Choudhury *et al.*, "Silver nanoparticles: Advanced and promising technology in diabetic wound therapy," *Mater. Sci. Eng. C*, vol. 112, no. February, p. 110925, 2020, doi: 10.1016/j.msec.2020.110925.
- [18] W. Zhu, H. Huang, Y. Dong, C. Han, X. Sui, and B. Jian, "Multi-walled carbon nanotube-based systems for improving the controlled release of insoluble drug dipyridamole," *Exp. Ther. Med.*, pp. 4610–4616, 2019, doi: 10.3892/etm.2019.7510.
- [19] A. I. A. Abd El-Mageed, M. Handayani, Z. Chen, T. Inose, and T. Ogawa, "Assignment of the Absolute-Handedness Chirality of Single-Walled Carbon Nanotubes Using Organic Molecule Supramolecular Structures," *Chem. - A Eur. J.*, vol. 25, no. 8, pp. 1941–1948, 2019, doi: 10.1002/chem.201804832.
- [20] B. Ribeiro, R. B. Pipes, M. L. Costa, and E. C. Botelho, "Electrical and rheological percolation behavior of multi-walled carbon nanotube-reinforced poly(phenylene sulfide) composites," *J. Compos. Mater.*, vol. 51, no. 2, pp. 199–208, 2017, doi: 10.1177/0021998316644848.
- [21] H. Sadegh *et al.*, "Synthesis of MWCNT-COOH-Cysteamine composite and its application for dye removal," *J. Mol. Liq.*, vol. 215, pp. 221–228, 2016, doi: 10.1016/j.molliq.2015.12.042.
- [22] S. Paliwal, K. Pandey, S. Pawar, H. Joshi, and N. Bisht, "A review on carbon nanotubes: As a nano carrier drug delivery system," *Indian J. Pharm. Sci.*, vol. 82, no. 5, pp. 766–772, 2020, doi: 10.36468/pharmaceutical-sciences.704.
- [23] J. Simon, E. Flahaut, and M. Golzio, "Overview of carbon nanotubes for biomedical applications," *Materials (Basel)*, vol. 12, no. 4, pp. 1–21, 2019, doi: 10.3390/ma12040624.
- [24] A. Kavosi *et al.*, "The toxicity and therapeutic effects of single-and multi-wall carbon nanotubes on mice breast cancer," *Sci. Rep.*, vol. 8, no. 1, pp. 1–12, 2018, doi: 10.1038/s41598-018-26790-x.
- [25] R. A. Sobh, H. E. S. Nasr, and W. S. Mohamed, "Formulation and in vitro characterization of anticancer drugs encapsulated chitosan/multi-walled carbon nanotube nanocomposites," *J. Appl. Pharm. Sci.*, vol. 9, no. 8, pp. 32–40, 2019, doi: 10.7324/JAPS.2019.90805.
- [26] Z. Khatti, S. M. Hashemianzadeh, and S. A. Shafiei, "A molecular study on drug delivery system based on carbon nanotube compared to silicon carbide nanotube for encapsulation of platinum-based anticancer drug," *Adv. Pharm. Bull.*, vol. 8, no. 1, pp. 163–167, 2018, doi: 10.15171/apb.2018.020.
- [27] Q. Yang *et al.*, "Exploiting the synergetic effects of graphene and carbon nanotubes on the mechanical properties of bitumen composites," *Carbon N. Y.*, vol. 172, no. October, pp. 402–413, 2021, doi: 10.1016/j.carbon.2020.10.020.
- [28] M. Jagannatham, P. Chandran, S. Sankaran, P. Haridoss, N. Nayan, and S. R. Bakshi, "Tensile properties of carbon nanotubes reinforced aluminum matrix composites: A review," *Carbon N. Y.*, vol. 160, pp. 14–44, 2020, doi: 10.1016/j.carbon.2020.01.007.
- [29] H. He, L. A. Pham-Huy, P. Dramou, D. Xiao, P. Zuo, and C. Pham-Huy, "Carbon nanotubes: Applications in pharmacy and medicine," *Biomed Res. Int.*, vol. 2013, pp. 1–12, 2013, doi: 10.1155/2013/578290.
- [30] N. M. Latiff, X. Fu, D. K. Mohamed, A. Veksha, M. Handayani, and G. Lisak, "Carbon based copper (II) phthalocyanine catalysts for electrochemical CO₂ reduction: Effect of carbon support on electrocatalytic activity," *Carbon N. Y.*, vol. 168, pp. 245–253, 2020, doi: 10.1016/j.carbon.2020.06.066.
- [31] H. Hu, T. Zhang, S. Yuan, and S. Tang, "Functionalization of multi-walled carbon nanotubes with phenylenediamine for enhanced CO₂ adsorption," *Adsorption*, vol. 23, no. 1, pp. 73–85, 2017, doi: 10.1007/s10450-016-9820-y.
- [32] R. S. Singh and K. Chauhan, *Functionalization of multi-walled carbon nanotubes for enzyme immobilization*, 1st ed., vol. 630. Elsevier Inc., 2020.
- [33] E. A. Mwafy and A. M. Mostafa, "Multi walled carbon nanotube decorated cadmium oxide nanoparticles via pulsed laser ablation in liquid media," *Opt. Laser Technol.*, vol. 111, no. July 2018, pp. 249–254, 2019, doi: 10.1016/j.optlastec.2018.09.055.
- [34] N. Sezer and M. Koç, "Oxidative acid treatment of carbon nanotubes," *Surfaces and Interfaces*, vol. 14, pp. 1–8, 2019, doi: 10.1016/j.surfint.2018.11.001.
- [35] L. Shahriary, R. Nair, S. Sabharwal, and A. A. Athawale, "One-step synthesis of Ag-reduced graphene oxide-multiwalled carbon nanotubes for enhanced antibacterial activities," *New J. Chem.*, vol. 39, no. 6, pp. 4583–4590, 2015, doi: 10.1039/c4nj02275k.
- [36] A. Subagio, E. Prihastanti, and Ngadiwiyana, "Application of functionalized multi-walled carbon nanotubes for growth enhancement of mustard seed germination," *Indones. J. Chem.*, vol. 20, no. 1, pp. 120–129, 2020, doi: 10.22146/ijc.41340.
- [37] N. X. Dinh, N. Van Quy, T. Q. Huy, and A. T. Le, "Decoration of silver nanoparticles on multi-walled carbon nanotubes: Antibacterial mechanism and ultrastructural analysis," *J. Nanomater.*, vol. 2015, no. i, pp. 1–11, 2015, doi: 10.1155/2015/814379.
- [38] Y. Yusof, M. I. Zaidi, and M. R. Johan, "Enhanced Structural, Thermal, and Electrical Properties of Multi-walled Carbon Nanotubes Hybridized with Silver Nanoparticles," *J. Nanomater.*, vol. 2016, pp. 1–9, 2016, doi: 10.1155/2016/6141496.